

Optical absorption and electronic band structure first-principles calculations of α -glycine crystals

M. Z. S. Flores, V. N. Freire, R. P. dos Santos, and G. A. Farias

Departamento de Física, Universidade Federal do Ceará, Caixa Postal 6030, 60455-900 Fortaleza, Ceará, Brazil

E. W. S. Caetano

Centro Federal de Educação Tecnológica do Ceará, Avenida 13 de Maio, 2081, Benfica, 60040-531 Fortaleza, Ceará, Brazil

M. C. F. de Oliveira

Departamento de Química Orgânica e Inorgânica, Universidade Federal do Ceará, Campus do Pici, 60451-970 Fortaleza, Ceará, Brazil

J. R. L. Fernandez and L. M. R. Scolfaro

Instituto de Física, Universidade de São Paulo, Caixa Postal 66318, 05315-970 São Paulo, São Paulo, Brazil

M. J. B. Bezerra, T. M. Oliveira, G. A. Bezerra, and B. S. Cavada

Departamento de Bioquímica, Laboratório de Bioquímica Molecular, Universidade Federal do Ceará, Campus do Pici, 60455-900 Fortaleza, Ceará, Brazil

H. W. Leite Alves

Departamento de Ciências Naturais, UFSJ, Caixa Postal 110, 36300-000 São João Del Rei, Minas Gerais, Brazil

(Received 26 March 2007; revised manuscript received 8 October 2007; published 4 March 2008)

Light absorption of α -glycine crystals grown by slow evaporation at room temperature was measured, indicating a 5.11 ± 0.02 eV energy band gap. Structural, electronic, and optical absorption properties of α -glycine crystals were obtained by first-principles quantum mechanical calculations using density functional theory within the generalized gradient approximation in order to understand this result. To take into account the contribution of core electrons, ultrasoft and norm-conserving pseudopotentials, as well as an all electron approach were considered to compute the electronic density of states and band structure of α -glycine crystals. They exhibit three indirect energy band gaps and one direct Γ - Γ energy gap around 4.95 eV. The optical absorption related to transitions between the top of the valence band and the bottom of the conduction band involves O $2p$ valence states and C, O $2p$ conduction states, with the carboxyl group contributing significantly to the origin of the energy band gap. The calculated optical absorption is highly dependent on the polarization of the incident radiation due to the spatial arrangement of the dipolar glycine molecules; in the case of a polycrystalline sample, the first-principles calculated optical absorption is in good agreement with the measurement when a rigid energy shift is applied.

DOI: [10.1103/PhysRevB.77.115104](https://doi.org/10.1103/PhysRevB.77.115104)

PACS number(s): 71.20.Rv, 78.20.-e, 78.40.Me, 78.55.Kz

I. INTRODUCTION

The crystals formed from the 20 natural amino acids are interesting structures, being intermediary between molecules and the conventional solid state. These amino acid crystals are stabilized by hydrogen bonds and dipolar electrostatic interactions (known as salt bridges).¹ Since the hydrogen bonds determine the spatial arrangement of the amino acid molecules in their crystalline form, they can also have an important role in the structural, electronic, and optical properties of amino acid crystals. There are efforts to take advantage of amino acid films in biosensors and optoelectronic devices,² and the adhesion of amino acids on a series of inorganic surfaces including insulators and semiconductors was already investigated.³ Oda and Nakayama^{4,5} have proposed to control electrically the amino acid ionization and the conformation of proteins arranged on semiconductor surfaces, which might produce new types of biodevices. Strosio and Dutta⁶ have described advances in man-made nanostructures integrated with biological molecules and systems, their properties, characteristics, and functions. Consequently, it is of paramount importance to understand fundamental as-

pects (in particular, electronic and optical characteristics) of amino acid crystals and films for the future development of bio-optoelectronic devices.

The crystal structures of several amino acids have been widely studied by x-ray diffraction and their vibrational (infrared and Raman) properties have also been measured. However, their luminescence and light absorption properties were not investigated in general, and information concerning electronic and optical properties of amino acid crystals is very limited. The unique exceptions are the pioneer luminescence and optical transmission studies below 3.5 eV in crystalline L-alanine, irradiated or doped with Cu and Fe performed by Winkler *et al.*⁷⁻⁹ In the case of Cu-doped L-alanine crystals, they have used nine Ar⁺-laser lines (514.5–454.5 nm) to show a broad luminescence in the visible region ($\hbar\omega > 3.0$ eV), which was attributed to defect states in the L-alanine crystal gap, but without any calculation of the band structure to strengthen such interpretation. Winkler *et al.*⁹ have also observed intense absorption in the ultraviolet range ($\hbar\omega > 3.4$ eV), and two other weaker absorptions in the visible region ($\hbar\omega \sim 2.0$ eV, 3.25 eV). Their results suggested that the L-alanine crystal is an insulator,

with energy gap in the ultraviolet energy range ($E_g > 4.0$ eV). This suggestion was confirmed by the light absorption and/or ultraviolet photoluminescence measurements and density functional theory calculations of Caetano *et al.*,² which have demonstrated that the L-alanine crystal is a wide direct gap material with $E_{g(\Gamma-\Gamma)} = 5.02$ eV. Later, Tulip and Clark¹ have investigated the structural and electronic properties of alanine, leucine, isoleucine, and valine crystals using density functional theory (DFT) within the generalized gradient approximation (GGA), finding energy band gaps of the order of 5.0 eV. In the case of L-alanine crystals, the calculations of Tulip and Clark¹ agree with both the experimental and theoretical results of Caetano *et al.*² However, their results could not be confirmed for leucine, isoleucine, and valine crystals due to lack of experimental data. Tulip and Clark¹ found that (i) the electrons are highly localized at the amino acid molecules in their crystals, (ii) the main mechanisms behind amino acid crystal formation and stabilization are dipolar electrostatic interactions and hydrogen bonding, and (iii) amine and carboxyl functional groups are crucial to determine the electronic band structure.

With the exception of L-alanine, leucine, isoleucine, and valine crystals,^{1,2} the electronic and optical properties of other amino acid crystals, to the best of our knowledge, were not investigated using *ab initio* methods. In particular, the optical properties of glycine crystalline polymorphs were not measured nor estimated by calculations. The theoretical study of observed and hypothetical polymorphs of glycine recently published by Chisholm *et al.*¹⁰ aimed to investigate the merits of crystal structure prediction using first-principles methods, and has focused only on their structural characteristics, without presenting data on their electronic structure and interactions with electromagnetic waves. Perlovich *et al.*¹¹ carried out x-ray, differential scanning calorimetry, and solution calorimetric investigations for α , β , and γ modifications of glycine, also presenting a survey of lattice parameters measured by several groups. Experimental results on the electronic and optical properties of glycine polymorph crystals are absent in the literature.

Although being the simplest amino acid, glycine [see the molecule in Fig. 1(a)] is essential for the biosynthesis of nucleic acids,¹² and acts as inhibitory neurotransmitter in the brain and/or spinal cord.^{13,14} It has no stereoisomers, but eight neutral minimum-energy conformers in the gas phase were predicted by theoretical studies,¹⁵ three of which being confirmed experimentally.^{16,17} In the solid state, glycine assumes the zwitterionic form $\text{NH}_3^+\text{CH}_2\text{COO}^-$, with three polymorphs α (monoclinic, $P2_1/n$), β (monoclinic, $P2_1$), and γ (hexagonal, $P3_2/P3_1$). While γ is more stable at room temperature,^{18,19} the α polymorph grows spontaneously from aqueous solutions and it is the most studied. In the α structure, layers of dipolar glycine molecules occur parallel to the ac plane due to two $\text{N-H}\cdots\text{O}$ hydrogen bonds. These layers are linked by much weaker bifurcated $\text{N-H}\cdots\text{O}$ hydrogen bonds and very weak interlayer $\text{C-H}\cdots\text{O}$ hydrogen bonds [see Figs. 1(b) and 1(c)], giving rise to antiparallel double layers.^{20,21}

The purpose of this work is to present light absorption experimental data for α -glycine crystals, as well as first-

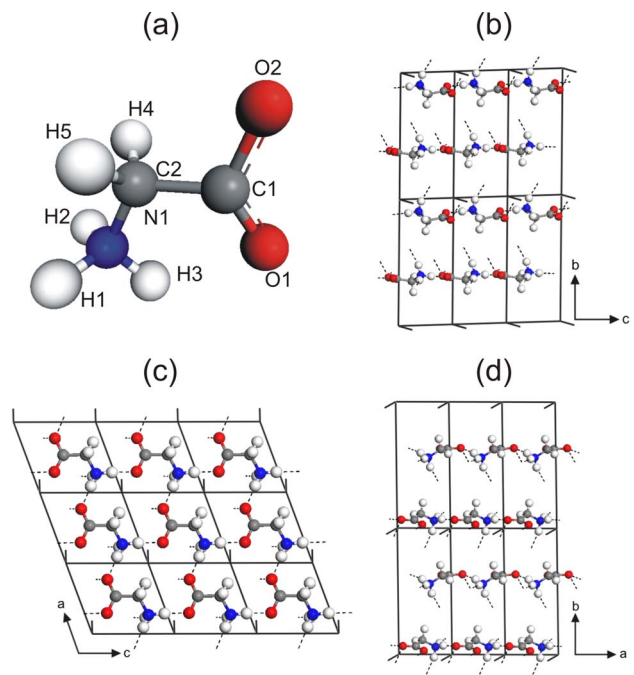


FIG. 1. (Color online) (a) The zwitterionic glycine molecule: C2 is the α -carbon; (b) hydrogen bonds in a α -glycine crystal depicted along the axis a ; (c) hydrogen bonds in a α -glycine crystal depicted along the axis b ; (d) hydrogen bonds in a α -glycine crystal depicted along the axis b . The amine and carboxyl groups are aligned along the $[001]$ axis.

principles quantum mechanical calculations of the electronic band structure, density of states, and optical absorption within the DFT-GGA in order to interpret the measurements. α -glycine crystals were grown by slow evaporation, and the best samples were used to perform the experiments. Experimental optical absorption indicates the existence of an inter-band energy gap of 5.11 ± 0.02 eV, which is close to the calculated electronic band structure of α -glycine crystals. An all electron (AE) approach, as well as ultrasoft pseudopotential (USP) and norm-conserving (NC) pseudopotential were used to compute the electronic band structure and density of states of α -glycine crystals, the former exhibiting three principal indirect gaps at different symmetry points, and one direct gap. Considering the all electron approach, the indirect energy gaps are 4.89, 4.94, and 4.96 eV, and the direct Γ - Γ energy gap is 4.95 eV. The optical absorption regime for energies below 5.3 eV is demonstrated to be ruled by transitions involving O $2p$ valence states and C, O $2p$ conduction states. The DFT-GGA estimated optical absorption is shown to be highly dependent on the polarization of the incident radiation due to the spatial arrangement of the zwitterionic (dipolar) glycine molecules.

The paper is organized as follows: in Sec. II, the growth and optical absorption measurements of α -glycine crystals are described; details of the quantum mechanical DFT-GGA calculations are presented in Sec. III, together with the electronic band structure obtained using ultrasoft and norm-conserved pseudopotentials, and an all electron framework; in Sec. IV, the theoretical optical absorption (which is compared with our measurements) for α -glycine crystals is cal-

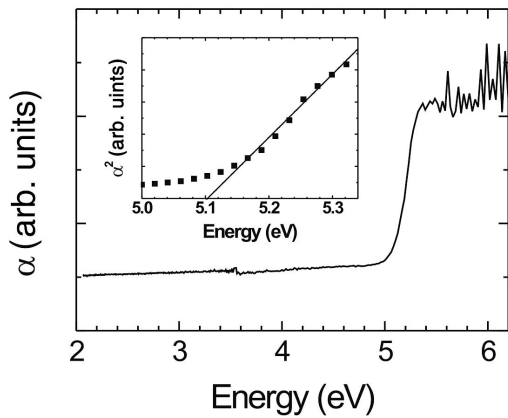


FIG. 2. Optical absorption of α -glycine crystals measured at 300 K with nonpolarized incident radiation. In the inset, the experimental data are depicted by squares, and the straight line points to the estimated energy gap.

culated within the pseudopotential scheme and taking into account the core electrons; the last section contains our concluding remarks.

II. OPTICAL ABSORPTION MEASUREMENT IN α -GLYCINE CRYSTALS

There are four glycine molecules (40 atoms) per unit cell in α -glycine crystals. The lattice parameters were obtained from x-ray diffraction by Perlovich *et al.*,¹¹ and Legros and Kvick.²² We have used the standard slow evaporation method to grow monoclinic ($P2_1/n$) α -glycine crystals at room temperature from saturated aqueous mother solutions of glycine (commercial, 99% pure, Sigma-Aldrich Corporation). The crystals of better optical quality were chosen for the measurements.

Light absorption measurements on five glycine crystal samples at 300 K were performed using a Carry 500 scan-Varian UV-vis-NIR photospectrometer, which has a 0.1 nm tolerance in the UV-visible spectrum. Figure 2 depicts a typical light absorption spectrum of α -glycine crystals, while the inset shows the optical absorption data evaluated over five samples. The light absorption of glycine crystals increases strongly around 5.11 eV, which is an estimate of the energy gap E_g of α -glycine crystals. The onset of the absorption coefficient α as a function of the energy for a direct band gap material is related to the incident photon energy by $\alpha = C(h\nu - E_g)^{1/2}$, where C is a constant.^{23,24} As the optical absorption in a direct optical transition is much stronger, we assume that the onset of the measured optical absorption spectrum is better described by using the formula for the optical absorption of a direct band gap material since the theoretical indirect and direct energy band gaps for glycine are very close, as demonstrated in the next section. In the region where the light absorption of α -glycine crystals increases strongly, a linear fit of the high energy side of the square of the absorbance presented in Fig. 2 indicates an energy gap of 5.11 ± 0.02 eV. The estimated error is related to the inhomogeneity and defects of the crystals due to the growth process.

III. BAND STRUCTURE OF α -GLYCINE CRYSTALS

In order to interpret the light absorption obtained experimentally, quantum mechanical first-principles calculations were carried out by using the density functional theory within the generalized gradient-corrected approximation (CASTEP code)²⁵ to obtain the lattice parameters and atomic internal coordinates of α -glycine crystals that minimize the unit cell total energy. The unit cell geometry and atomic positions of the α -glycine crystal were optimized using experimental x-ray data¹¹ as input for our calculations. The Perdew-Burke-Ernzerhof (PBE) exchange-correlation functional²⁶ was used in the GGA approach, while Vanderbilt ultrasoft pseudopotentials were adopted to represent core electrons. Evaluation of integrals in the reciprocal space was achieved using a (5,2,5) Monkhorst-Pack grid,²⁷ which corresponds to a k -point separation of about 0.04 \AA^{-1} . The Broyden-Fletcher-Goldfarb-Shanno optimization scheme was adopted and a plane-wave basis set was used to represent the electronic states. In order to obtain an atomic geometry that minimizes the unit cell total energy, lattice parameters, unit cell angles, and atomic positions were converged obeying the following criteria: (i) total energy variation smaller than 5×10^{-6} eV, (ii) maximum force on any atom smaller than 0.01 eV/\AA , (iii) stress smaller than 0.02 GPa , and (iv) atomic displacements smaller than $5 \times 10^{-4} \text{ \AA}$. The converged lattice parameters calculated with cutoff energy $E_{cut} = 560 \text{ eV}$ are in good agreement with those obtained by Chisholm *et al.*,¹⁰ as well as with the experimental values of Legros and Kvick,²² and Perlovich *et al.*¹¹

After geometry optimization with $E_{cut} = 560 \text{ eV}$ and always adopting the PBE exchange-correlation functional, the electronic band structure and the density of states (total, partial, and the relative contribution of each atom) of α -glycine crystals were evaluated in three different ways using (i) the same ultrasoft pseudopotentials and plane-wave basis set of the geometry optimization, with cutoff energy 560 eV ; (ii) norm-conserved pseudopotentials²⁸ with cutoff energy of 770 eV for the plane-wave basis set; and (iii) double numerical plus polarization orbitals,^{29,30} considering explicitly all electrons (core+valence) with a cutoff radius of 5 \AA , and a self-consistent total energy convergence threshold of 10^{-6} eV/at . The choice of norm-conserved pseudopotentials for the optical property calculations was made because ultrasoft pseudopotentials produce a contribution to optical matrix elements that is not included in the CASTEP code (however, ultrasoft calculated optical properties are generally in good agreement with the results obtained using norm-conserving potentials).

The atomic and functional group contributions to the density of states are shown in Fig. 3. There are four energy bands close to -20 eV originating mainly from O $2s$ orbitals, but with a contribution of C $2s$ orbitals; 8 bands near -17.5 eV with main contributions from O $2s$ and N $2s$ orbitals (known as lone pairs); and 4 bands near -12.0 eV with main contribution from C $2s$ orbitals. In the energy region between -8.0 and -2.5 eV there are 32 valence bands with contributions from O $2p$, C $2p$, and N $2p$ orbitals. The 12 uppermost valence bands in the -1.3 to 0.0 eV range result mostly from O $2p$ orbitals. For the lowest conduction bands

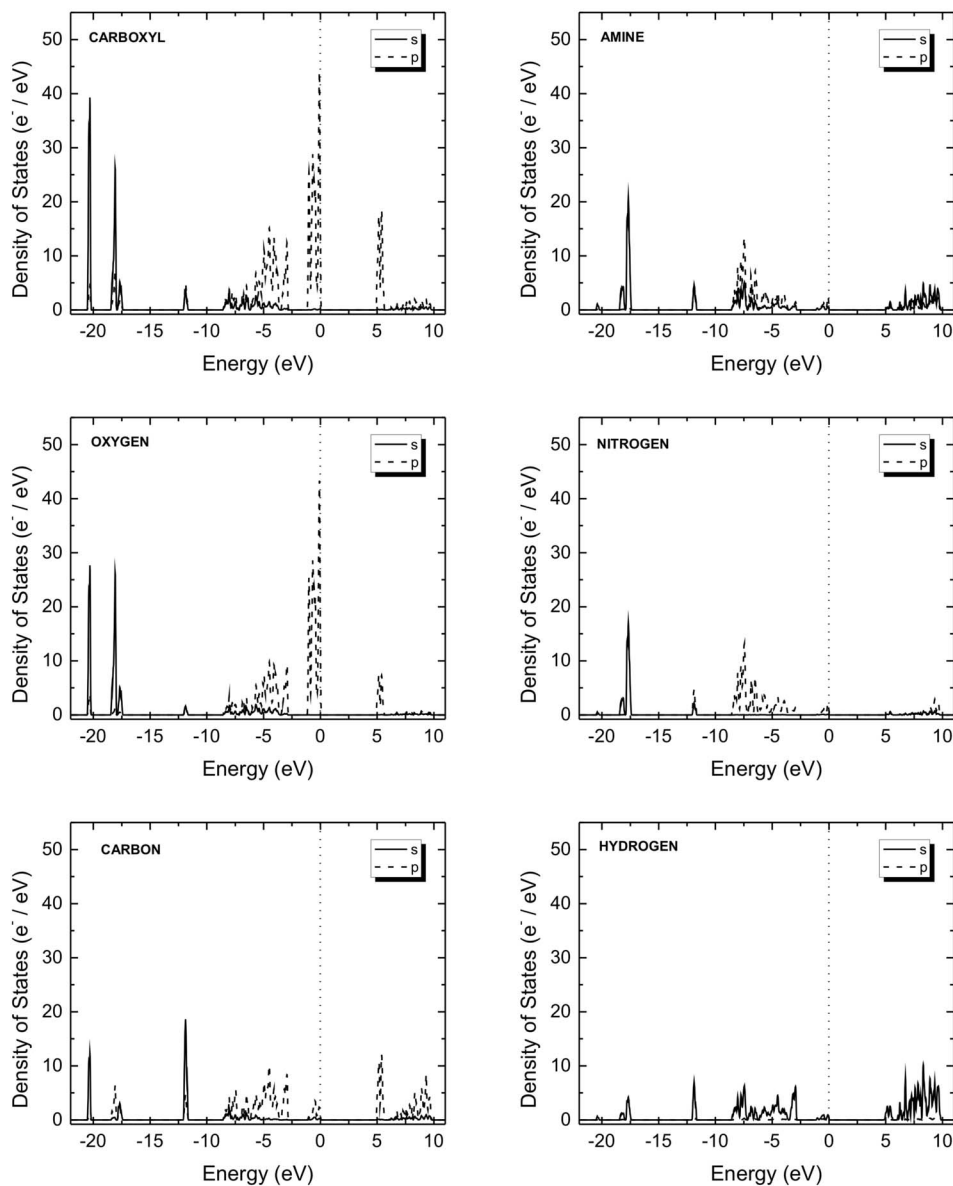


FIG. 3. Atomic and functional group contributions to the density of states of α -glycine monoclinic crystals calculated within the all electron approach.

around 5.11 eV, the main contributions are from C $2p$ and O $2p$ orbitals, but there is a slight contribution of the H $1s$ states from the amine site. Finally, the most important contribution for the partial density of states above 6.0 eV comes from unoccupied H $1s$ states. In terms of functional groups, it is the carboxyl one that contributes more significantly to the highest valence and lowest conduction bands which give rise to the 5.11 eV main energy gap, as shown clearly at the top, left side panel of Fig. 3. This result contrasts with the suggestion of Tulip and Clark¹ that the carboxyl and amine functional groups are dominant in determining the band structure of L-alanine, -leucine, -isoleucine, and -valine crystals. Such difference is, however, too small and must be accounted for due to numerical fluctuations during the computations carried out by us and those of Tulip and Clark.¹ We also suppose that the existence of quasidegenerated bands

and the small size of the plane wave basis set adopted in both works help us to explain this difference.

The full electronic band structure of α -glycine crystals is shown in Fig. 4, which was obtained using the all electron approach. Details of the band structure close to the main gap are shown in Fig. 5. In the case of the valence band, all approaches (AE, NC, and USP) lead to practically the same band structure (differences smaller than 10 meV). This occurs because DFT is well suited to describe ground state properties. There are three valence band maxima located between the symmetry points Z and Γ , Y and A, and B and D. Their energies calculated within the different approaches are shown in Table I. Figure 5 shows that the AE (solid lines), USP (dotted lines), and NC calculations (dashed lines) predict decreasing values for the conduction band minimum. A rigid vertical energy shift of 0.31 eV for $E_{NC} \rightarrow E_{AE}$ and

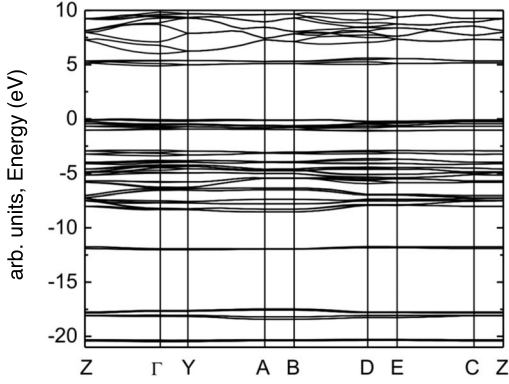


FIG. 4. Band structure of α -glycine monoclinic crystals in the -20.0 to 10 eV range calculated within the all electron approach.

0.17 eV for $E_{US} \rightarrow E_{AE}$ leaves all three approaches with quite approximately the same conduction band curves. Through our calculations, we find that α -glycine crystals have three close indirect energy gaps in different symmetry points whose values are shown in Table I. When double numerical plus polarization orbitals are considered to obtain the electronic band structure, the indirect gaps are 4.89 eV ($[Z, \Gamma] \rightarrow \Gamma$), 4.94 eV ($[Y, A] \rightarrow \Gamma$), and 4.96 eV ($[B, D] \rightarrow \Gamma$), while the direct gap ($\Gamma \rightarrow \Gamma$) is 4.95 eV. Both valence band maxima and conduction band minima are originated for the most part from O $2p$ orbitals of the carboxyl group $-\text{COOH}$, as shown by the density of states depicted in Fig. 3.

Due to the well known underestimation of band gaps in DFT calculations, the α -glycine crystal must have an insulator character with a band gap larger than 4.95 eV, which is in close agreement with the 5.11 ± 0.02 eV obtained from the optical absorption measurements (see Fig. 2). The difference between theoretical calculations and the experimental value is of the order of -10% for the band structure calculated within the norm-conserved approach, and of the order of -3% for the band structure calculated using the all electron approach, an unexpected level of agreement for DFT calculations, which usually underestimate the band gap by 30% – 50% .

TABLE I. Valence band maxima (three first lines of the table) and band gap energies (four remaining lines) for α -glycine crystal calculated within the all electron, ultrasoft, and norm-conserving pseudopotential approaches.

	AE (eV)	US (eV)	NC (eV)
$[Z, \Gamma]$	0.000	0.000	0.000
$[Y, A]$	-0.056	-0.062	-0.055
$[B, D]$	-0.073	-0.076	-0.074
$[Z, \Gamma] \rightarrow \Gamma$	4.89	4.74	4.58
$[Y, A] \rightarrow \Gamma$	4.94	4.80	4.63
$[B, D] \rightarrow \Gamma$	4.96	4.81	4.65
$\Gamma \rightarrow \Gamma$	4.95	4.81	4.64

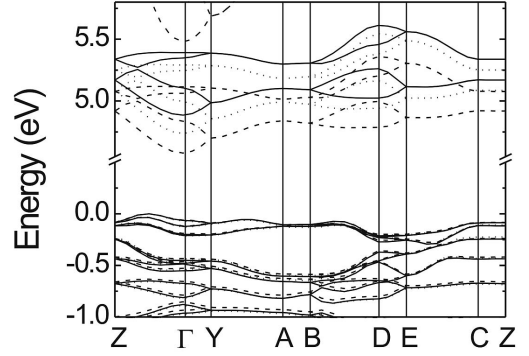


FIG. 5. Detail of the band structure of α -glycine near the Fermi energy level. The curves were obtained from calculations considering the all electron approach (solid lines), and ultrasoft (dotted lines) and norm-conserving pseudopotentials (dashed lines).

IV. CALCULATED OPTICAL ABSORPTION OF α -GLYCINE CRYSTALS

The optical absorption was calculated from the oscillator strengths computed for interband transitions involving the norm-conserved pseudopotential electronic wave functions, and considering incident light polarized along the $[001]$, $[100]$, and $[010]$ crystalline axes and a polycrystalline sample. The optical absorption was obtained from the imaginary part of the complex dielectric function, given by

$$\varepsilon_2(\omega) = \frac{2e^2\pi}{\Omega\varepsilon_0} \sum_{\mathbf{k}, v, c} |\langle \psi_{\mathbf{k}}^c | \hat{\mathbf{u}} \cdot \mathbf{r} | \psi_{\mathbf{k}}^v \rangle|^2 \delta(E_{\mathbf{k}}^c - E_{\mathbf{k}}^v - \hbar\omega), \quad (1)$$

where ω is the light frequency, and $\psi_{\mathbf{k}}^c$ and $\psi_{\mathbf{k}}^v$ are, respectively, the conduction and valence band wave functions at \mathbf{k} calculated within the DFT-GGA approach. The vector $\hat{\mathbf{u}}$ points along the polarization of the incident electric field. The real part ε_1 of the dielectric function is obtained from the imaginary part ε_2 using the Kramers-Kronig relationship.^{31,32} The imaginary and real parts of the refraction index (k and n , respectively) are related to ε_1 and ε_2 through

$$\varepsilon_1 = n^2 - k^2, \quad (2)$$

$$\varepsilon_2 = 2nk. \quad (3)$$

Finally, the optical absorption has the following expression:

$$I(\omega) = \frac{2k\omega}{c}. \quad (4)$$

Looking at Fig. 6, the optical absorption for light polarized along $[100]$ is much more pronounced within the 4.5 – 7.5 eV energy range. On the other hand, the absorption regime for energies below 5.3 eV, which includes indirect and direct electronic transitions assigned in the band structure shown in Fig. 5, has small peaks. Looking at the partial density of states, we note that this regime is ruled by transitions involving O $2p$ valence and conduction states. These transitions are precluded due to the orbital angular momentum selection rule. Indeed, the optical absorption is due to

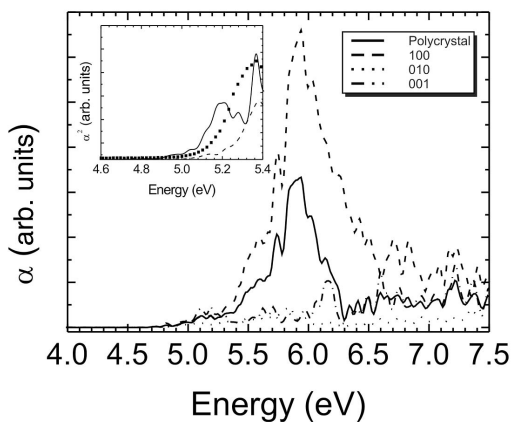


FIG. 6. Optical absorption calculated with norm-conserving pseudopotentials for different polarization planes ([100]—dashed; [010]—dotted; [001]—dash dotted) and a polycrystalline sample (solid). The inset shows a comparison between the square of the experimental absorbance (squares), and the squared optical absorption calculated for polycrystalline samples using ultrasoft (solid) and norm-conserved (dashed) pseudopotentials.

the coupling of electronic states via an electric dipole interaction term, which is small when electronic states originated from atomic orbitals with the same angular quantum number are considered.

For energies in the 5.3–6.3 eV range, there is a strong peak for absorption along the [100] direction in comparison with absorption along the [010] and [001] directions. The partial density of states reveals a strong contribution from N $2p$ levels to the electronic wave functions therein. To explain this, we remember that oxygen atoms are situated in one side of the glycine molecule, at the carboxyl group, while nitrogen is part of the amine group on the opposite side. In the α -glycine crystal, amine and carboxyl groups in a same molecule are almost aligned to the [001] axis, as shown in Fig. 1(b). However, there is some interaction between neighbor molecules. Looking at one positively charged amine group and its three negatively charged carboxyl nearest neighbors in the ac plane, it can be seen that the electric dipole that results by adding the dipole components along the lines connecting the amine to the carboxyl radicals has a dominating component along [100]. So, for incident light polarized along the [100] crystal axis a strong electric dipole coupling emerges that transfers charge from carboxyl groups to amine groups, strengthening the absorption peak we observe in our theoretical calculations. A direct electronic transition, on the other hand, explains the energy value where the strongest absorption peak takes place, as commented below. Therefore, absorption for a polycrystalline sample will be mainly due to the [100] contribution.

For energies larger than 6.3 eV, the absorption intensity decreases for all polarization directions because O $2p$ levels contribute more intensely to the conduction states above this energy. The main polycrystalline absorption peaks occur for 5.3, 5.5, 5.8, 5.9 (strongest), and 6.1 eV. The first two peaks

are related to indirect transitions from the top of the valence band to the two conduction bands above 5.2 eV. The strongest peak is related to direct transitions ($\Gamma \rightarrow \Gamma$) involving the minimum of the conduction band near 5.9 eV (see Fig. 5). The inset of Fig. 6 shows a direct comparison between the square of the experimental absorbance and the calculated square of the absorption coefficient. It is a well known fact that in a direct band gap solid, the squared absorbance increases linearly for energies close to the energy gap. As we have shown, indirect and direct energy gaps in glycine are too close, and therefore the smaller indirect gap must be masked when one looks at the onset of optical absorption,²⁴ which is practically dominated by $\Gamma \rightarrow \Gamma$ transitions for energies a few tenths of meV larger than the minimum indirect energy gap. The curves were scaled independently to be compared. We can see clearly that the rise of the optical absorption occurs for smaller energies in the theoretical curve in comparison to the experimental data, which is due to the underestimate of the energy gap in DFT computations.

V. CONCLUDING REMARKS

Our first-principles DFT-GGA calculations indicate that the α -glycine crystal is an indirect gap material, with an energy gap of 5.11 ± 0.02 eV as measured in this work by optical absorption. However, α -glycine crystals present three very close indirect and one direct energy gap, as demonstrated by our first-principles calculations. This result can be compared, for example, with the direct energy gap suggested for L-alanine crystals,^{1,2} indicating that not only the spatial arrangement of the amino acid molecules in the crystal, but also the type of lateral chain is important to determine whether the energy gap of an amino acid crystal is direct or indirect. Two absorption regimes, for energies smaller than 5.3 eV and in the 5.3–6.3 eV range, were obtained in our calculations. In the first regime, which involves transitions mainly from O $2p$ valence to O $2p$ conduction states, selection rules related to the wave function angular momentum preclude optical absorption, which exhibits only small peaks for light with different incident polarizations. In the second regime, O $2p$ valence to N $2s$ conduction states are involved, and a strong electric dipole coupling with carboxyl and amine groups along the [100] direction, which explains the strong absorption for incident radiation with that polarization. The strong absorption peak at 5.9 eV is due to a direct transition ($\Gamma \rightarrow \Gamma$) from the valence band to the minimum of the fifth conduction band close to 5.9 eV.

ACKNOWLEDGMENTS

V.N.F., G.A.F., L.M.R.S., B.S.C., and H.W.L.A. are senior researchers of the Conselho Nacional de Pesquisa Científica e Desenvolvimento Tecnológico (CNPq) in Brazil. V.N.F., G.A.F., and B.S.C. received financial support from project CNPq-Rede NanoBioestruturas, No. 555183/2005-0. T.M.O., G.A.B., R.P.d.S., and M.Z.S.F. received support from CNPq during the development of this work.

- ¹P. R. Tulip and S. J. Clark, Phys. Rev. B **71**, 195117 (2005).
- ²E. W. S. Caetano, M. Z. S. Flores, G. A. Bezerra, J. R. Pinheiro, V. N. Freire, G. A. Farias, J. R. L. Fernandez, J. R. Leite, M. C. F. de Oliveira, J. A. Pinheiro, B. S. Cavada, J. L. de Lima Filho, and H. W. Leite Alves, AIP Conf. Proc. **772**, 1095 (2005).
- ³R. L. Willett, K. W. Baldwin, K. W. West, and L. N. Pfeiffer, Proc. Natl. Acad. Sci. U.S.A. **102**, 7817 (2005).
- ⁴M. Oda and T. Nakayama, Appl. Surf. Sci. **244**, 627 (2005).
- ⁵M. Oda and T. Nakayama, Jpn. J. Appl. Phys., Part 1 **45**, 8939 (2006).
- ⁶M. A. Stroschio and M. Dutta, Proc. IEEE **93**, 1772 (2005).
- ⁷E. Winkler, P. Etchegoin, A. Fainstein, and C. Fainstein, Phys. Rev. B **57**, 13477 (1998).
- ⁸E. Winkler, A. Fainstein, P. Etchegoin, and C. Fainstein, Phys. Rev. B **59**, 1255 (1999).
- ⁹E. Winkler, P. Etchegoin, A. Fainstein, and C. Fainstein, Phys. Rev. B **61**, 15756 (2000).
- ¹⁰J. A. Chisholm, S. Motherwell, P. R. Tulip, S. Parsons, and S. J. Clark, Cryst. Growth Des. **5**, 1437 (2005).
- ¹¹G. L. Perlovich, L. K. Hansen, and A. Bauer-Brandl, J. Therm. Anal. Calorim. **66**, 699 (2001).
- ¹²Molecular expression: The Amino Acid Collection, in <http://micro.magnet.fsu.edu/aminoacids/pages/glycine.html>
- ¹³S. M. Paul, Gaba and Glycine, in *Psychopharmacology: The Fourth Generation of Progress*, edited by F. E. Bloom and D. J. Kupfer (Raven Press, New York, 1995), pp. 87–94.
- ¹⁴R. A. Davidoff, R. P. Shank, L. T. Graham, Jr., M. H. Aprison, and R. Werman, Nature (London) **214**, 680 (1967).
- ¹⁵G. M. Chaban, J. O. Jung, and R. B. Gerber, J. Phys. Chem. A **104**, 10035 (2000).
- ¹⁶K. Iijima, K. Tanaka, and S. Onuma, J. Mol. Struct. **246**, 257 (1991).
- ¹⁷P. D. Godfrey and R. D. Brown, J. Am. Chem. Soc. **117**, 2019 (1995).
- ¹⁸H. Sakai, H. Hosogai, T. Kawakita, K. Onuma, and K. Tsukamoto, J. Cryst. Growth **116**, 421 (1992).
- ¹⁹N. Doki, M. Yokota, K. Kido, S. Sasaki, and N. Kubota, Cryst. Growth Des. **4**, 103 (2004).
- ²⁰E. S. Boek, D. Feil, W. J. Briels, and P. Bennema, J. Cryst. Growth **114**, 389 (1991).
- ²¹C. Murli, S. M. Sharma, S. Karmakar, and S. K. Sikka, Physica B **233**, 339 (2003).
- ²²J. O. Legros, and Å. Kvik, Acta Crystallogr., Sect. B: Struct. Crystallogr. Cryst. Chem. **36**, 3052 (1980).
- ²³H. Y. Fan, Rep. Prog. Phys. **19**, 107 (1956).
- ²⁴A. M. Fox, *Optical Properties of Solids*, 1st ed. (Oxford University Press, Oxford, 2001), p. 58–60.
- ²⁵M. D. Segall, P. J. D. Lindan, M. J. Probert, C. J. Pickard, P. J. Hasnip, S. J. Clark, and M. C. Payne, J. Phys.: Condens. Matter **14**, 2717 (2002).
- ²⁶J. P. Perdew, K. Burke, and M. Ernzerhof, Phys. Rev. Lett. **77**, 3865 (1996).
- ²⁷H. J. Monkhorst and J. D. Pack, Phys. Rev. B **13**, 5188 (1976).
- ²⁸G. J. Ackland, Phys. Rev. Lett. **80**, 2233 (1998).
- ²⁹B. Delley, J. Chem. Phys. **92**, 508 (1990).
- ³⁰B. Delley, J. Chem. Phys. **113**, 7756 (2000).
- ³¹H. A. Kramers, Nature (London) **117**, 775 (1926).
- ³²R. de L. Kronig, J. Opt. Soc. Am. **12**, 547 (1926).